Reference in J. Chem. Phys. style:

P. K. Das, D. W. Dockter, D. R. Fahey, D. E. Lauffer, G. D. Hawkins, J. Li, T. Zhu, C. J. Cramer, D. G. Truhlar, S. Dapprich, R. D. J. Froese, M. C. Holthausen, Z. Liu, K. Mogi, S. Vyboishchikov, D. G. Musaev, and K. Morokuma, in *Transition State Modeling for Catalysis*, edited by D. G. Truhlar and K. Morokuma (American Chemical Society Symposium Series Volume 721, Washington, DC, 1999), pp. 208–224.

Reference in Am. Chem. Soc. style:

Das, P. K.; Dockter, D. W.; Fahey, D. R.; Lauffer, D. E.; Hawkins, G. D.; Li, J.; Zhu, T.; Cramer, C. J.; Truhlar, D. G.; Dapprich, S.; Froese, R. D. J.; Holthausen, M. C.; Liu, Z.; Mogi, K.; Vyboishchikov, S.; Musaev, D. G.; K. Morokuma, K. In *Transition State Modeling for Catalysis*, Truhlar, D. G., Morokuma, K., Eds.; ACS Symposium Series 721; American Chemical Society: Washington, DC, 1999; pp. 208–224.

Chapter 17

Ethylene Polymerization by Zirconocene Catalysis

P. K. Das[1], D. W. Dockter[1], D. R. Fahey[1], D. E. Lauffer[1], G. D. Hawkins[2], J. Li[2], T. Zhu[2], C. J. Cramer[2], Donald G. Truhlar[2], S. Dapprich[3], R. D. J. Froese[3], M. C. Holthausen[3], Z. Liu[3], K. Mogi[3], S. Vyboishchikov[3], D. G. Musaev[3], and K. Morokuma[3]

[1]Phillips Petroleum Company, 327 PL PRC, Bartlesville, OK 74004
[2]Department of Chemistry, University of Minnesota, 207 Pleasant Street S.E., Minneapolis, MN 55455
[3]Cherry L. Emerson Center for Scientific Computation and Department of Chemistry, Emory University, Atlanta, GA 30322

The production of polyethylene by zirconocene catalysis is a multistep process that includes initiation, propagation, and termination. Each of these steps has a number of associated equilibrium and transition state structures. These structures have been studied in the gas-phase environment using density functional and integrated methods. We have also examined the effects of solvation upon the energetics of the various polymerization steps employing continuum and explicit representations of the solvent (toluene). The reaction steps we have studied are initiation, propagation, propylene and hexene incorporation, termination by hydrogenolysis, termination by β-H transfer to the metal, termination by β-H transfer to the monomer, and reactivation. The solvation effect of toluene takes on special significance for the initiation, termination by hydrogenolysis and by β-H transfer to the metal, and reactivation steps.

Owing to their high commercial interest as catalysts for olefin polymerization, the group IVA metallocenes have been the subject of many recent quantum-chemical studies *(1-29)*. For the most part, these studies have focused on the insertion of ethylene into metallocenium cations (considered to be the active catalyst species). Attention has also been given to termination steps in the polymerization scheme, namely, those involving β-hydride transfer from the growing polymer chain to the metal center and to the monomer in the monomer/metallocenium-cation complex. To the best of our knowledge, hydrogenolysis has not been investigated as a termination step in previous work, although hydrogen is a commonly used chain terminating agent

for molecular weight control. In addition, all of the previous computational work deals with the gas phase; the role of a solvent on the energetics of the various steps in the polymerization scheme is addressed here for the first time.

In this paper, we present results from our computational studies of various relevant reaction steps involving two zirconocene catalyst systems, namely, Cp_2ZrR^+ (System I) and $[CpCH_2Cp]ZrR^+$ (System II) where R denotes H or an alkyl group. The reaction steps considered in this study are shown in Scheme A. While most of the results came from the application of full high level (full-HL) density functional methodology, in one case we have tested an integrated method (IMOMO) that uses high-level MO calculations for the reaction part and lower-level MO calculations for the spectator part of a molecule. Moreover, using two recently developed solvation models, we have computed the effect of toluene as a solvent on the reaction steps of Scheme A, as mediated by the two zirconocene catalysts.

Computation Methodologies

All full-HL computations (energetics, optimized geometries and analytical second derivatives) were performed using the B3LYP hybrid density functional theory method (*30*) that incorporates Becke's 3-parameter hybrid exchange *(31)* and Lee-Yang-Parr correlation functionals *(32,33)*. The full-HL calculations were carried out with the following basis sets (*34*): LANL2DZ with a relativistic effective core potential (RECP) for Zr, LANL2DZ for the other atoms involved in the reaction center (H or alkyl groups bonded to Zr and coordinated olefins), and 3-21G for C and H atoms of the auxiliary ligands (L_1 and L_2, see Scheme A). Optimized equilibrium geometries and transition states (TSs) were obtained using non-redundant internal coordinates starting with Hessians calculated at the restricted Hartree-Fock (RHF) level. Analytical second derivatives (*35*) were used to obtain the frequencies for the enthalpies and free energies (scale factor = 1.0) and to verify minima and TSs.

The integrated method (*36-39*), IMOMO, is similar to that of the integrated molecular orbital molecular mechanics (IMOMM) method that has been described earlier in the literature (*40,41*), the difference being that the force-field treatment of the spectator portion of the molecule is replaced by a lower-level molecular orbital method. The notation IMOMO(HL:LL) will be used to designate an IMOMO calculation, where HL and LL denote the high-level and low-level MO methods, respectively. IMOMO HL energies and optimized geometries were calculated using the B3LYP method with the basis set described above; whereas the LL energies and geometries were obtained using the RHF method with the following basis sets (*34d-g*): LANL1MB with RECP for Zr and LANL1MB for the other atoms. No frequencies were calculated at the IMOMO level. All full-HL and IMOMO calculations were performed using either GAUSSIAN 94 or the developmental version GAUSSIAN 95 (*42,43*).

The two solvation models used in this work, namely, SM5.2R/MNDO/d and SM5.42R/BPW91/MIDI!(6D), are implemented in the codes, AMPAC5.4m1 (*44*) and DGAUSS4.0m1 (*45*), respectively. They are based on extensions of the SM5 suite of solvation models (*46-49*) to organometallic complexes of zirconium. The SM5 suite is an extension of earlier SMx models (*50-52*) that were originally implemented in the AMSOL (*53*) program.

Scheme A: Polymerization Reaction Steps

Reaction steps **2-5** involving the catalyst systems Cp_2ZrR^+ (System I) and $[CpCH_2Cp]ZrR^+$ (System II), with R = H or an alkyl group, were studied.

1: Catalyst Activation (Not investigated in this study)

$$[L_1,L_2]ZrCl_2 + \text{Cocatalyst} \rightarrow [L_1,L_2]ZrCH_3^+ + \text{Cocatalyst}^-$$

2: Initiation

$$[L_1,L_2]ZrCH_3^+ + CH_2{=}CH_2 \rightarrow \pi\text{-complex} \rightarrow TS \rightarrow [L_1,L_2]ZrCH_2CH_2CH_3^+$$

3a, 3a': Propagation

$$[L_1,L_2]ZrCH_2CH_2CH_3^+ + CH_2{=}CH_2 \rightarrow \pi\text{-complex} \rightarrow TS \rightarrow [L_1,L_2]ZrCH_2CH_2CH_2CH_2CH_3^+$$

3a: Ethylene approaching from the front side of the alkyl chain.

3a': Ethylene approaching from the back side of the alkyl chain.

3b: Comonomer incorporation

$$[L_1,L_2]ZrCH_2CH_2CH_3^+ + CH_2{=}CHR' \rightarrow \pi\text{-complex} \rightarrow TS \rightarrow [L_1,L_2]ZrCH_2CH(R')CH_2CH_2CH_3^+$$

R' = CH_3 for propylene incorporation

R' = C_4H_9 for 1-hexene incorporation

4a, 4a' & 4a'': Termination by hydrogenolysis

$$[L_1,L_2]ZrR^+ + H_2 \rightarrow \pi\text{-complex} \rightarrow TS \rightarrow [L_1,L_2]ZrH(RH)^+ \rightarrow [L_1,L_2]ZrH^+ + RH$$

4a: R = CH_3

4a': R = $CH_2CH_2CH_3$, H_2 approaching from the front side of the alkyl chain

4a'': R = $CH_2CH_2CH_3$, H_2 approaching from the back side of the alkyl chain

4b: Termination by β-H transfer to metal center

$$[L_1,L_2]ZrCH_2CH_2CH_3^+ \rightarrow TS \rightarrow [L_1,L_2]ZrH(CH_2{=}CHCH_3)^+ \rightarrow [L_1,L_2]ZrH^+ + CH_2{=}CHCH_3$$

4c: Termination by β-H transfer to monomer in the complex

$$[L_1,L_2]ZrCH_2CH_2CH_3^+ + CH_2{=}CH_2 \rightarrow \pi\text{-complex} \rightarrow TS \rightarrow$$
$$[L_1,L_2]ZrCH_2CH_3(CH_2{=}CHCH_3)^+ \rightarrow [L_1,L_2]ZrCH_2CH_3^+ + CH_2{=}CHCH_3$$

5: Reactivation

$$[L_1,L_2]ZrH^+ + CH_2{=}CH_2 \rightarrow \pi\text{-complex} \rightarrow TS \rightarrow [L_1,L_2]ZrCH_2CH_3^+$$

Notations and Definitions

ΔE^c, ΔH^c, and ΔG^c Energy, enthalpy, and free energy change for the complexation substep (applicable to all reaction steps above, except **4b**).

ΔE^r, ΔH^r, and ΔG^r Energy, enthalpy, and free energy change for the reaction substep, measured from the complex except for **4b** where it is measured from the reactant cation.

$\Delta E^{\ddagger}$, $\Delta H^{\ddagger}$, and $\Delta G^{\ddagger}$ Activation energy, activation enthalpy, and activation free energy for the reaction substep, referenced from the π-complex except for **4b** where it is referenced from the reactant cation.

ΔE^s, ΔH^s, and ΔG^s Energy, enthalpy, and free energy change for the separation substep (applicable to termination steps, **4a-a''**, **b**, **c**, above)

Born-Oppenheimer energies without ZPE will be denoted as E, and enthalpies and free energies for gas-phase processes at temperature, T, will be denoted as H_T and G_T, respectively. All solution-phase free energies correspond to a concentration of 1 mol L^{-1} and a temperature of 298 K and are denoted as G_S. Except for **4b**, each reaction step includes a reaction substep, r, that usually starts at the π-complex and ends at the product complex; the reaction substep for reaction step **4b** starts at the reactant cation and ends with the product complex. Also, each reaction step except for **4b** includes a complexation substep, c, preceding the reaction substep. All termination reaction steps, **4a-a''**, **b**, and **c**, include a separation substep, s, in which the product of the reaction substep separates.

The standard-state solvation energy, ΔG_S^0, of a solute molecule is computed as the sum of three terms, namely: (1) the gain, G_P, in electric polarization energy due to the polarization of the solvent; (2) the energy cost, ΔE_{EN}, for distorting the electronic/nuclear structure of the solute to be self-consistent with the polarized solvent; and (3) the contribution, G_{CDS}, to the free energy of solvation due to cavity formation, dispersion interactions, solvent structural changes, and other effects of the first solvation shell that differ from those included in G_P. Thus,

$$\Delta G_S^0 = \Delta E_{EN} + G_P + G_{CDS}. \quad (1)$$

The sum of G_P and ΔE_{EN} is determined by a self-consistent reaction field calculation (*49*, *54*) and depends on the solvent dielectric constant. In the present work the nuclear relaxation part of ΔE_{EN} is not included explicitly, but rather it is included implicitly in the parameterization of the CDS terms. G_{CDS} is calculated from empirical atomic surface tension coefficients and the solvent-accessible surface area (SASA) of the solute. In particular G_{CDS} is a sum of atomic contributions of the form $\sigma_k A_k$, where σ_k is the surface tension of atom k and A_k is the exposed area of atom k.

Two models, SM5.2R/MNDO/d (*48*) and SM5.42R/BPW91/MIDI!(6D) (*49*), that were originally parameterized and tested against 2,135 experimental solvation free energy data for 275 neutral solutes, 49 ions, and 91 solvents (*48,49*) were adapted here to specifically treat zirconium compounds in toluene at room temperature. Since no experimental data were available for the free energy of solvation of any zirconium solute, an indirect route was used to develop the atomic surface tension coefficient (σ_{Zr}) needed for computing the contribution of the Zr atom to G_{CDS} in toluene. First, a free energy cycle was constructed as shown in Figure 1. In this cycle, M is a Zr-containing cation, T is a toluene molecule, C is a complex of M with a single toluene molecule, g stands for gas-phase, and s stands for toluene solution. $\Delta G_S^0(M)$, $\Delta G_S^0(T)$, and $\Delta G_S^0(C)$ are the solvation free energies in toluene for M, T, and C, respectively; and ΔG_T^c and ΔG_S^c are the complexation free energies in the gas phase and in solution, respectively. The key to the method is that ΔG_S^c should be zero because it simply corresponds to labeling the first-solvation-shell of toluene in two different ways, first as part of the solvent, then as part of the solute. This gives the following equation:

$$\Delta G_S^0(M) + \Delta G_S^0(T) = \Delta G_T^c + \Delta G_S^0(C). \quad (2)$$

In principle, both $\Delta G_S^0(M)$ and $\Delta G_S^0(C)$ contain the contributions to the CDS energies from Zr. An examination of three-dimensional space-filling models of the complexes as well as an estimate of the solvent-accessible surface area of Zr in the complexes indicate that the zirconium atom in the complex is totally buried, i.e., the Zr contribution to CDS should be zero for the complex; therefore, we chose the solvent radius large enough (1.7 Å) to insure that A_{Zr} is zero for four complexes of interest. (Note that a solvent radius of zero is used for computing A_k for a non-metallic

atom k in SM5.2R.) The atomic surface tension, σ_{Zr}, for Zr thus can be determined in the following way:

$$\sigma_{Zr} A_{Zr}(\mathrm{M}) = \Delta G_{\mathrm{T}}^{\mathrm{c}} + \Delta G_{\mathrm{S}}^{0}(\mathrm{C}) - \Delta \tilde{G}_{\mathrm{S}}^{0}(\mathrm{M}) - \Delta G_{\mathrm{S}}^{0}(\mathrm{T}), \tag{3}$$

where $A_{Zr}(\mathrm{M})$ is the exposed surface area of Zr in M, and $\Delta \tilde{G}_{S}^{0}(\mathrm{M})$ is the solvation free energy for M without a first-solvation shell contribution from Zr. The Zr atomic surface tensions for two specific solvation models described below were obtained using

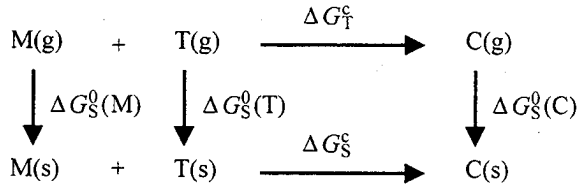

Figure 1. Free energy cycle used in developing the solvation models

Equation 3 and the gas-phase free energies for $Cp_2ZrCH_3^+$ and $Cp_2ZrCH_3(C_6H_5CH_3)^+$ (Figure 2A and Table I). These parameterizations were then tested using Equation 2 and the gas-phase free energies for the three zirconocenium cations, Cp_2ZrR^+ and the cation-toluene complexes, $Cp2ZrR(C_6H_5CH_3)^+$, with R = H, Cl, and $CH_2CH_2CH_3$.

Some important features of the two specific solvation models for Zr compounds in toluene (henceforth referred to as zirconium solvation models, ZSM1 and ZSM2) are given below.

ZSM1: Semiempirical method implemented with the MNDO/d parameters of Thiel et al. *(55-58)* except for the Zr α parameter that was optimized to 1.4 $Å^{-1}$.

Fixed (Rigid) solute geometries: We used optimized gas-phase geometries for the solute geometries. The contribution to E_{EN} from nuclear relaxation was absorbed in the CDS term.

Charge model: We used Mulliken charges (Class II charges) to compute G_P.

First-solvation-shell term: We used SM5-type surface tension functional forms *(46-49)* to compute G_{CDS}. For toluene, the surface tension coefficients were determined by the solvent properties, namely, index of refraction of 1.4961, hydrogen-bond acidity of 0.0, hydrogen-bond basicity of 0.14, and macroscopic surface tension of 40.2 cal mol^{-1} $Å^{-2}$.

ZSM2: DFT method implemented with the BPW91 (*59*) exchange-correlation functional; for Zr, DGAUSS-built-in valence basis sets PPC (atomic) and AP1 (fitting) were used with pseudopotentials. For the other atoms, the MIDI! basis set (*60*) was used with the original five-function spherical harmonic *d* set replaced by a six-function Cartesian *d* set.

Fixed (Rigid) solute geometries: We used the same geometries as for ZSM1.

Charge model: We used Class IV CM2 charges (*61*), mapped from Löwdin population analysis, to compute G_P. In previous validation studies (*61*), the mapping was found to decrease the errors in dipole moments, typically by a factor of 3. Special attention was paid to obtaining realistic charges for aromatics.

First-solvation-shell term: We used parameters similar to those in ZSM1.

For the free energies of activation, adding the solvation energies at the gas-phase stationary points corresponds to the assumption of separable equilibrium solvation (*62*).

Results and Discussion

a. Specific Binding of Toluene to Zirconocenium Cations. In general, toluene may coordinate to the transition metal center of the zirconocenium cations in several different ways, i.e., via η^1(one C atom), η^2 (two C atoms), η^3 (three C atoms), η^6 (six C atoms), or its methyl-group. Two zirconocenium cation-toluene conformers, η^1 and pseudo-η^3, are shown in Figures 2A and 2B, respectively. We note also, although not

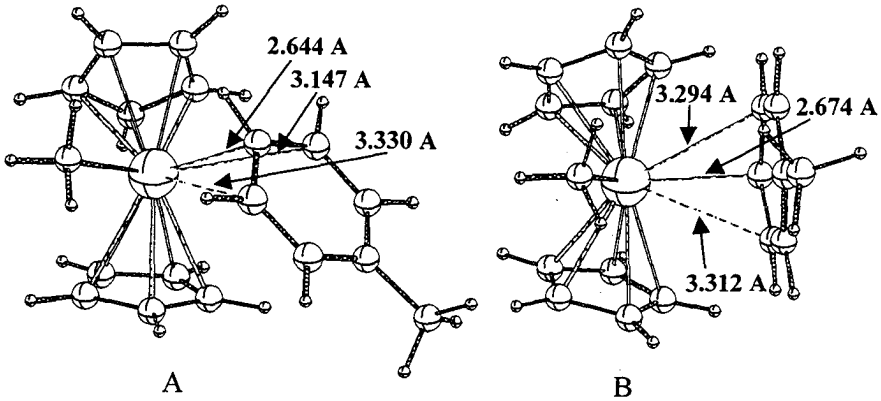

E = -742.847535 a.u. *E* = -742.843921 a.u.

Figure 2. Structures of stable complexes of toluene with $Cp_2ZrCH_3^+$

shown in the figure, that the ethylene molecule is coordinated to the zirconocenium cations in a slightly asymmetric-η^2 manner. The difference between the coordination of the toluene and that of ethylene may be due to the relatively strong repulsive steric interactions of a toluene molecule with the auxiliary ligands. In Figure 2A, we show the lowest-energy conformer, having values of -22.1 and -10.3 kcal/mol for ΔH°_{298} and ΔG°_{298}, respectively. These numbers are only slightly larger (1-2 kcal/mol) than

the corresponding values for ethylene coordination to the zirconocenium cations. Table I gives the complexation energies for Cp_2ZrR^+ with R= H, Cl, CH_3, and $CH_2CH_2CH_3$ and shows that toluene does bond strongly to zirconocenium cations. All of the energies listed in Table I correspond to those of the most stable conformers with structures similar to Figure 2A.

b. Gas-Phase Full-HL Calculations Ethylene Insertion. For the reaction steps in Scheme A, full-HL computations have been performed for the gas-phase stationary points on the potential energy surface. The classical energetics, i.e., the electronic contributions (including nuclear repulsion) without zero point energies (ZPE), are summarized in Table II. Overall, there are significant differences in energetics between

Table I. Full-HL gas-phase energetics (kcal/mol) of the complexation of toluene with zirconocenium cations.

Zirconocenium cation	ΔE^c	ΔH^c_{298}	ΔG^c_{298}
Cp_2ZrH^+	-27.8	-25.5	-14.9
Cp_2ZrCl^+	-25.0	-22.0	-12.0
$Cp_2ZrCH_3^+$	-24.7	-22.1	-10.3
$Cp_2ZrCH_2CH_2CH_3^+$			
β-agostic	-14.1	-11.4	0.1
almost non-agostic	-24.2	-21.6	-9.6

Table II. Energetics (kcal/mol) for the reaction steps involving $[CpCH_2Cp]ZrR^+$ and Cp_2ZrR^+

Reaction step[a]	$[CpCH_2Cp]ZrR^+$				Cp_2ZrR^+			
	ΔE^c	ΔE^r	$\Delta E^{\neq}$	ΔE^s	ΔE^c	ΔE^r	$\Delta E^{\neq}$	ΔE^s
2	-21.6	-7.7	7.1		-19.8	-8.1	6.5	
3a	-14.7	-9.7	6.0		-9.5	-9.9	3.5	
3a'	-14.7	-8.8	6.4		-10.8	-10.0	7.2	
3b	-16.9	-2.5	9.6		-13.8	-4.0	7.2	
4a	-7.8	-14.0	5.3	12.5	-7.8	-14.7	4.4	14.6
4a'	-6.6	-9.5	10.3	16.1	-3.9	-12.5	7.8	16.2
4a"	-8.5	-10.3	5.5	18.8	-6.0	-11.5	3.4	17.5
4b		10.9	12.0	26.9		12.5	12.3	25.0
4c	-14.7	-4.4	11.4	16.4	-9.5	-4.9	12.3	11.8
5	-24.7[b]	-15.6[b]	1.9[b]		-22.5[b]	-17.7[b]	1.6[b]	

[a]For numbering of steps and notation for energetics, see Scheme A.
[b]Ethylene is in a broad-side-on orientation.

the bridged and non-bridged zirconocene systems for the reaction steps under consideration. The reaction activation barriers ($\Delta E^{\neq}$) for propagation, hexene incorporation, and hydrogenolysis reaction steps are lower for the non-bridged system.

Since the zero point, thermal energetic, entropic, and solvation contributions to free energy changes play an important role in determining the energetics of the reaction steps, further examination of the reaction energetics will be deferred until solvent effects are discussed.

c. IMOMO(HL:LL) Calculations for Propylene Incorporation. IMOMO calculations were performed to test the adequacy of this method for modeling higher olefin insertion by using ethylene as a subsystem for the higher olefin homologues. The energies (ΔE) and geometries were calculated by IMOMO method for reaction step **3b**, where propylene was used as the comonomer. For the HL systems, we chose the homologous complexes $Cp_2Zr(C_2H_5)^+$ and $Cp_2Zr(C_4H_9)^+$ in which one methyl group in both the $Cp_2Zr(C_3H_7)^+$ and the propylene and two methyl groups in the π-complex, transition state, and products were replaced by hydrogen atoms. The reactants, intermediates, transition states, and products were calculated for a front side, 2,1-insertion, i.e., insertion by the addition of the metal alkyl to the coordinated propylene to give a secondary alkyl group attached to the metal. The potential energy surfaces and optimized geometries for this reaction, calculated at both the IMOMO and full-HL levels of theory, are presented in Figures 3 and 4, respectively.

Most of the IMOMO bond distances presented in Figure 4 are within 1% of those calculated using the full-HL method. In particular, the agostic interaction distances and carbon-zirconium bond distances shown in the figure are in good agreement with those optimized at full-HL level. The advantage of the IMOMO method is that it provides, at a lower cost, geometries comparable to those obtained from full-HL calculations. However, as Figure 3 shows, the differences in the energetics between the full-HL and the IMOMO calculations are as large as 3 kcal/mol. This suggests that caution should be used when applying this IMOMO approach to the calculation of energetics.

d. Solvation Effects. The modification of the gas-phase free energy changes by the solvent effect has been computed for all applicable substeps of the reaction steps in Scheme A, except step **1**. The data for the two zirconocene catalyst systems I and II are compiled in Table III, where we use the notation

$$\Delta\Delta G^{x} \equiv \Delta G^{x}_{S} - \Delta G^{x}_{298}, \quad x = c,\ r,\ s,\ \text{or}\ \neq. \tag{4}$$

The definitions of ΔG^{x}_{S} , ΔG^{x}_{298}, and the reaction substeps are given in Scheme A. Generally, the solvation models, ZSM1 and ZSM2, predict very similar solvation effects (to within ~1 kcal/mol) for the free energy changes of all reaction substeps, except for the hydrogenolysis reaction, where the unsigned differences in the $\Delta\Delta G^{x}$s between the two models for a given zirconium complex range from 1 to 4 kcal/mol.

Table IV shows enthalpy (ΔH^{x}_{298}) and free energy (ΔG^{x}_{298}, ΔG^{x}_{S}) changes for the reactions substeps involving systems I and II, respectively. To illustrate how the energetics change at the various stages of a reaction, energy diagrams for reaction steps **2, 3a, 4a''**, and **4b** involving $[CpCH_2Cp]ZrR^+$ are given in Figures 5-8. At this point in our gas-phase computational work, we have only identified saddle points for the reaction substep; the nature of the transition states (if any) for the complexation and

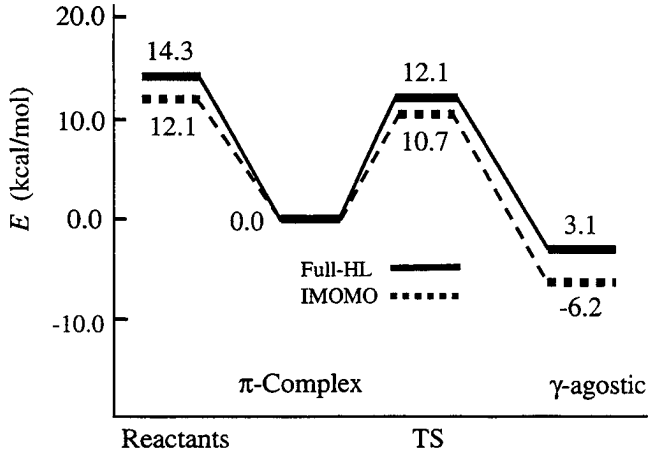

Figure 3. Energetics calculated at the IMOMO and full-HL levels for the propylene incorporation step, **3b**: $Cp_2ZrCH_2CH_2CH_3^+ + CH_2{=}CHCH_3 \rightarrow Cp_2ZrCH_2CH(CH_3)CH_2CH_2CH_3^+$.

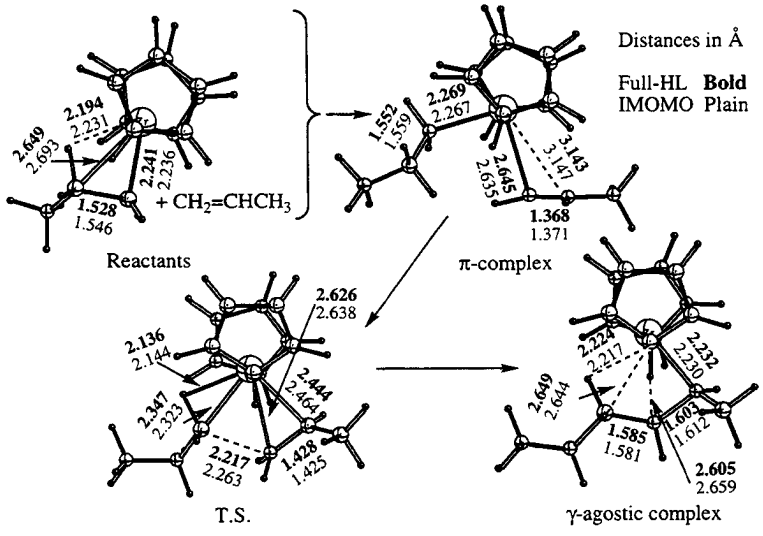

Figure 4. Optimized geometries of the reactants, intermediate, transition state, and product of the propylene incorporation reaction step, **3b**.

Table III. Solvent effects (kcal/mol) on free energy changes, upper entry computed by ZSM1 and lower entry computed by ZSM2.

Zirconocenium Cation	Reaction Step[a]	$\Delta\Delta G^c$	$\Delta\Delta G^r$	$\Delta\Delta G^{\neq}$	$\Delta\Delta G^s$
Cp_2ZrR^+	**2**	6.1	-0.1	-0.1	
		5.4	-0.4	0.5	
	3a	1.4	-0.6	-1.3	
		1.1	-0.5	-0.0	
	3a'	1.1	-0.4	0.1	
		1.1	-0.7	0.0	
	3b	1.7	0.6	0.9	
		2.2	0.5	0.9	
	4a	2.0	3.0	0.3	-9.6
		3.3	-0.4	0.3	-8.5
	4a'	-2.3	1.8	-1.0	-11.1
		-0.8	-1.6	-0.6	-10.0
	4a''	-3.3	3.1	1.1	-11.6
		-0.7	-1.0	0.1	-10.7
	4b		1.4	0.9	-11.3
			0.1	0.9	-10.5
	4c	1.4	0.2	0.0	-2.8
		1.1	0.1	0.2	-2.7
	5	10.1	-1.4	0.3	
		8.8	0.1	0.4	
$[CpCH_2Cp]ZrR^+$	**2**	9.9	-0.3	0.1	
		9.1	-0.4	0.6	
	3a	3.5	-0.5	-1.2	
		3.0	-0.6	-0.1	
	3a'	3.0	0.2	0.1	
		2.8	-0.2	0.1	
	3b	5.3	-0.6	-0.5	
		4.9	0.1	-0.1	
	4a	5.1	3.4	0.9	-14.9
		6.2	0.4	0.7	-13.7
	4a'	-0.3	2.1	-1.1	-17.0
		1.2	-1.2	-1.0	-15.8
	4a''	-1.1	2.9	1.3	-17.0
		1.0	-1.2	0.4	-15.7
	4b		3.2	1.4	-16.7
			2.3	1.8	-16.7
	4c	3.5	0.4	-0.1	-4.9
		3.0	0.2	0.1	-4.5
	5	15.4	-3.1	0.4	
		13.9	-2.0	0.8	

[a]For numbering of steps and notation for energetics, see Scheme A and Equation 4.

Table IV. Enthalpy and free energy changes in the gas phase and free energy changes in toluene for reaction steps involving Cp_2ZrR^+ (upper entry) and $[CpCH_2Cp]ZrR^+$ (lower entry).

Reaction Step[a, b]	ΔH^c_{298}	ΔG^c_{298}	ΔG^c_S	ΔH^r_{298}	ΔG^r_{298}	ΔG^r_S	$\Delta H^{\neq}_{298}$	$\Delta G^{\neq}_{298}$	$\Delta G^{\neq}_S$	ΔH^s_{298}	ΔG^s_{298}	ΔG^s_S
2	-18.1	-6.7	-0.6	-6.2	-3.4	-3.5	6.6	7.9	7.8			
	-20.2	-9.9	0.0	-5.8	-3.1	-3.4	7.1	10.1	10.2			
3a	-7.1	4.4	5.8	-9.0	-7.9	-8.5	2.9	4.5	3.2			
	-12.6	-1.2	2.3	-7.1	-5.3	-5.8	5.3	6.9	5.7			
3a'	-8.5	5.8	6.9	-8.9	-9.0	-9.4	7.7	9.6	9.7			
	-12.8	-1.0	1.0	-7.5	-6.8	-6.6	6.7	9.2	9.3			
3b	-11.3	0.8	2.5	-3.1	-2.4	-1.9	6.9	9.4	10.3			
	-15.0	-3.3	2.0	-1.3	0.5	-0.1	9.2	11.7	11.2			
4a	-5.9	1.4	3.4	-12.0	-11.5	-8.5	4.2	5.9	6.2	10.8	0.8	-8.9
	-6.2	1.1	6.2	-11.3	-11.6	-8.2	5.0	6.5	7.4	11.5	2.1	-12.8
4a'	-1.4	7.7	5.4	-10.3	-10.9	9.1	6.9	7.3	6.3	14.9	3.8	-7.3
	-4.6	3.2	2.9	-7.0	-9.5	-7.5	9.4	9.7	8.6	15.0	6.2	-10.8
4a''	-3.3	5.7	2.4	-9.3	-10.5	-7.4	2.7	3.3	4.4	16.0	4.4	-7.2
	-6.4	2.3	1.2	-8.0	-9.1	-6.2	4.9	5.1	6.4	17.7	6.6	-10.4
4b				10.9	11.5	12.9	9.6	10.5	11.4	23.3	10.7	-0.6
				9.2	8.4	11.6	9.4	9.5	10.9	25.5	13.9	-2.8
4c	-7.1	4.4	5.8	-4.9	-4.9	-4.7	9.9	12.6	12.6	9.5	-3.3	-6.1
	-12.6	-1.2	2.3	-4.5	-5.3	-4.9	8.9	11.4	11.3	14.2	3.5	-1.4
5	-20.8	-10.5	-0.4	-15.9	-15.1	-16.5	7.2	2.0	2.3			
	-23.3	-13.1	2.3	-13.8	-12.0	-15.1	1.3	2.5	2.9			

[a]Calculated by ZSM1. All data are in kcal/mol.

[b]For numbering of the steps and notation for energetics, see Scheme A.

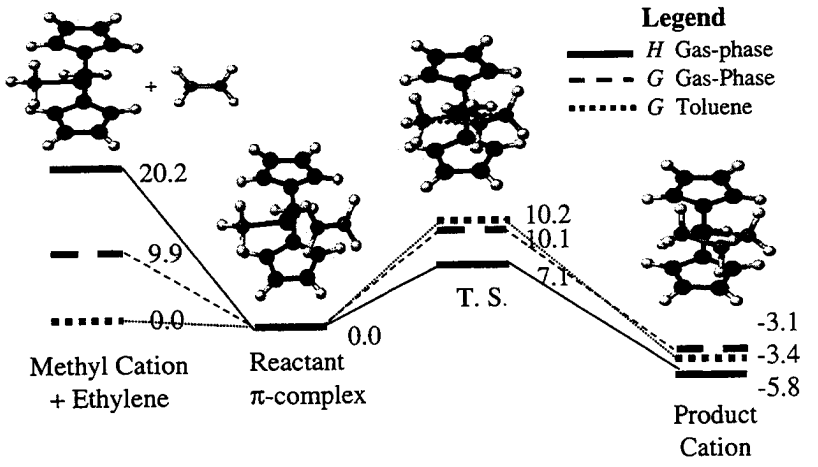

Figure 5. Relative enthalpies and free energies for the initiation reaction step, **2**. involving $[CpCH_2Cp]ZrCH_3^+ + C_2H_4$.

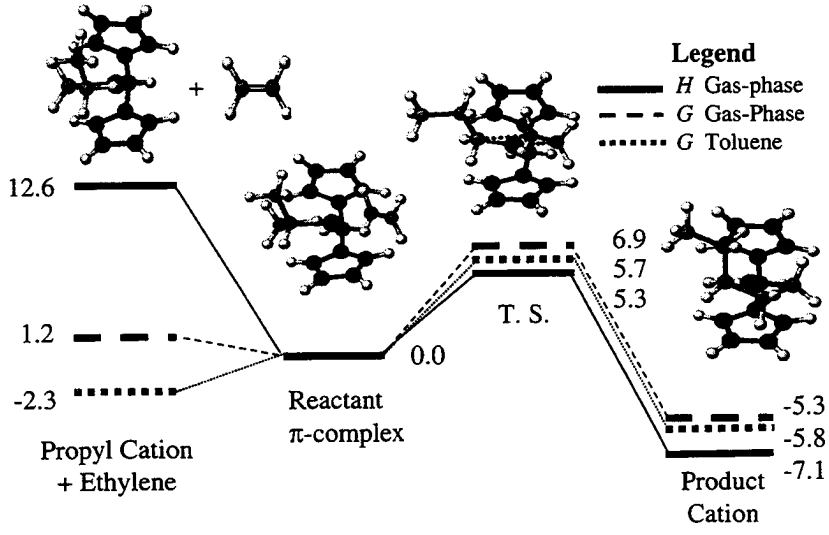

Figure 6. Relative enthalpies and free energies for the propagation reaction step, **3a**, involving $[CpCH_2Cp]ZrCH_2CH_2CH_3^+ + C_2H_4$.

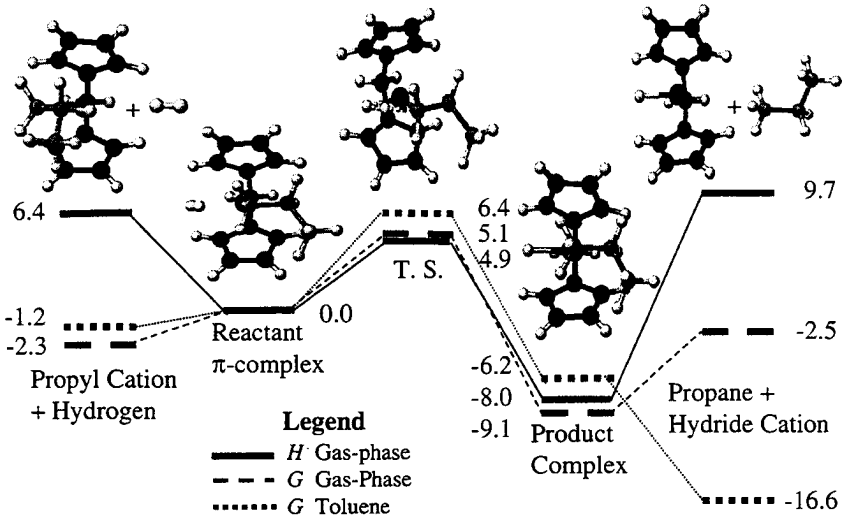

Figure 7. Relative enthalpies and free energies for the termination by hydrogenolysis reaction step, **4a**, involving $[CpCH_2Cp]ZrCH_2CH_2CH_3^+ + H_2$.

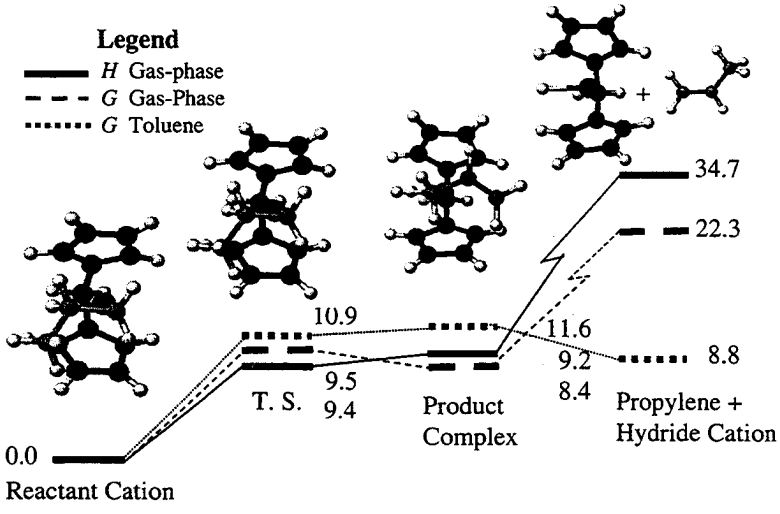

Figure 8. Relative enthalpies and free energies for the termination by β-H transfer to the metal center reaction step, **4b**, involving $[CpCH_2Cp]ZrCH_2CH_2CH_3^+$.

separation substeps is not clear. It is evident from the data in Table IV, as well as from Figures 5-8, that the greatest effect of the solvent is manifested in those substeps involving tri-coordinated zirconocenium cations, i.e., the complexation and separation substeps. The free energy changes and the activation free energies for the reaction substeps are changed to lesser extents in going from the gas phase to the solution phase. Also, we note that there is a significant difference in what is observed when one examines free energy changes rather than enthalpy changes.

The solvation effects are important in developing an understanding of the mechanisms involved in zirconcene-catalyzed ethylene polymerization. Specifically, solvation effects are pronounced in the initiation reaction step **2** (see Figure 5), the reactivation reaction step **5,** and the termination reaction steps **4a-a"** and **4b**, see Table III. Considering the case of the initiation reaction for $[CpCH_2Cp]ZrR^+$ without solvation, the transition state free energy is nearly the same (within 0.2 kcal/mol) as the free energy of the reactants, both referenced to the same energy level; but with solvation the former is 10 kcal/mol higher. For the termination reaction steps, solvation reduces the free energy changes for the separation into products by approximately 16 kcal/mol for reactions **4a-a"** and **4b**. Thus, predictions involving the energetics of polymerization mechanisms including these reactions are likely to depend significantly on solvation effects.

Solvation plays quite a different role in the free energies of activation for the two insertion steps, i.e., initiation and propagation. (Note that the free energy of activation for these reaction steps is $\Delta G^c + \Delta G^{\neq}$ if the reactants are in chemical equilibrium with the reactant complex.) The present gas-phase calculations (Figures 5 and 6) yield free energies of activation of 0.2 and 5.7 kcal/mol, respectively, for the initiation and propagation steps, referenced to separate reactants, implying that the latter provides a higher dynamical bottleneck. However, for a toluene solvent the calculations (also in Figures 5 and 6) yield 10.2 and 8.0 kcal/mol for corresponding free energies of activation for initiation and propagation, implying that the former provides a higher bottleneck and that the overall activation energy is about 10 kcal/mol. Thus the results of the condensed-phase calculations change our qualitative understanding of the polymer chain growth mechanism.

Summary and Conclusions

We have performed electronic structure and free energy of solvation calculations on two structurally distinct zirconocene catalyst systems. Comparing the two systems, significant differences are observed in the energetics at stationary points along the reaction paths for the various reaction steps involved in ethylene polymerization and hexene incorporation. Moreover, considering each zirconocene system separately, the changes in the gas-phase free energies and the solution-phase free energies differ significantly from each other. Two notable consequences for the catalyst systems studied are that the insertion reaction step is most likely the dynamical bottleneck for the polymer chain growth and that termination by β-H transfer to the metal center may indeed be a viable polymer chain termination process.

For large metallocene systems, the integrated method, IMOMO, shows promise for obtaining optimized geometries and possibly energies.

Acknowledgment

This work was performed in part under the support of the United States Department of Commerce, National Institute of Standards and Technology.

Literature Cited

1. Fujimoto, H.; Koga, N.; Fukui, K. *J. Am. Chem. Soc.* **1981**, *103*, 7452.
2. Fujimoto, H.; Yamasaki, T.; Mizutani, H.; Koga, N. *J. Am. Chem. Soc.* **1985**, *107*, 6157.
3. Fujimoto, H. *Acc. Chem. Res.* **1987**, *20*, 448.
4. Marynick, D. S.; Axe, F. U.; Hansen, L. M.; Jolly, C. A. *Topics in Physical Organometallic Chemistry;* Freund Publishing House: London, **1988**; Vol. 3, p. 37.
5. Shiga, A.; Kawamura, H.; Ebara, T.; Sasaki,, T.; Kikuzono, Y. *J. Organomet. Chem.* **1989**, *366*, 95.
6. Jolly, C. A.; Marynick, D. S. *J. Am. Chem. Soc.* **1989**, *111*, 7968.
7. Kawamura-Kuribayashi, H.; Koga, N.; Morokuma, K. *J. Am. Chem. Soc.* **1992**, *114*, 2359.
8. Kawamura-Kuribayashi, H.; Koga, N.; Morokuma, K. *J. Am. Chem. Soc.* **1992**, *114*, 8687.
9. Janiak, C. J. *Organomet. Chem.* **1993**, *63*, 452.
10. Bierwagen, E. P.; Bercaw, J. E.; Goddard, III, W. A. *J. Am. Chem. Soc.* **1994**, *116*, 1481.
11. Woo, T. K.; Fan, L.; Ziegler, T. *Organometallics* **1994**, *13*, 432.
12. Woo, T. K.; Fan, L.; Ziegler, T. *Organometallics* **1994**, *13*, 2252.
13. Axe, F. U.; Coffin, J. M. *J. Phys. Chem.* **1994**, *98*, 2567.
14. Meier, R. J.; Doremaele, G. H. J.; Iarlori, S.; Buda, F. *J. Am. Chem. Soc.* **1994**, *116*, 7274.
15. Weiss, H.; Ehrig, M.; Ahlrichs, R. *J. Am. Chem. Soc.* **1994**, *116*, 4919.
16. Sini, G.; Macgregor, S. A.; Eisenstein, O.; Teuben, J. H. *Organometallics* **1994**, *13*, 1049.
17. Fusco, R.; Longo, L. *Macromol. Theory Simul.* **1994**, *3*, 895.
18. Lohrenz, J. C. W.; Woo, T. K.; Ziegler, T. *J. Am. Chem. Soc.* **1995**, *117*, 12793.
19. Fan, L.; Harrison, D.; Woo, T. K.; Ziegler, T. *Organometallics* **1995**, *14*, 2018.
20. Lohrenz, J. C. W.; Woo, T. K.; Fan, L.; Ziegler, T. *J. Organomet. Chem.* **1995**, *497*, 91.
21. Fan, L.; Harrison, D.; Deng, L.; Woo, T. K.; Swehone, D.; Ziegler, T. *Can. J. Chem.* **1995**, *73*, 989.
22. Yoshida, T.; Koga, N.; Morokuma, K. *Organometallics* **1995**, *14*, 746.
23. Yoshida, T.; Koga, N.; Morokuma, K. *Organometallics* **1996**, *15*, 766.
24. Woo, T.; Margl, P. M.; Lohrenz, J. C. W.; Blöchl, P. E.; Ziegler, T. *J. Am. Chem. Soc.* **1996**, *118*, 4434.
25. Cruz, V. L.; Munoz-Escalona, A.; Martinez-Salazar, J. *Polymer* **1996**, *37*, 1663.
26. Margl, P.; Lohrenz, J. C. W.; Ziegler, T.; Blöchl, P. E. *J. Am. Chem. Soc.* **1996**, *118*, 4434.
27. Woo, T. K.; Margl, P. M.; Ziegler, T.; Blöchl, P. E. *Organometallics* **1997**, *16*, 3454.
28. Borve, K. J.; Jensen, V. R.; Karlsen, T.; Stovneng, J. A.; Swang, O. *J. Mol. Model.* **1997**, *3*, 193.
29. Fusco, R.; Longo, L.; Masi, F.; Garbassi, F. *Macromolecules* **1997**, *30*, 7673.
30. Stephens, P. J.; Devlin, F.J.; Chabalowski, C. F.; Frisch, M. J. *J. Phys. Chem.* **1994**, *98*, 11623.
31. Becke, A. D. *J. Chem. Phys.* **1993**, *98*, 5648.
32. Lee, C.; Yang, W.; Parr, R. G. *Phys. Rev. B* **1988**, *37*, 785.
33. Miehlich, B.; Savin, A.; Stoll, H.; Preuss, H. *Chem. Phys. Lett.* **1989**, *157*, 200.

34. (a) Binkley, J. S.; Pople, J. A.; Hehre, W.J. *J. Amer. Chem. Soc.* **1980**, *102*, 939.
(b) Gordon, M. S.; Binkley, J. S.; Pople, J. A.; Peitro, W. J.; Hehre, W. J. *J. Amer. Chem. Soc.* **1982** *104*, 2797.
(c) Pietro, W. J.; Francl, M. M.; Hehre, W. J.; Defrees, D. J.; Pople, J. A.; Brinkley, J. S. *J. Amer. Chem. Soc.* **1982**, *104*, 5039.
(d) Dunning, Jr. T. H.; Hay, P. J. in *Modern Theoretical Chemistry, Vol 3*; H. F. Schaefer, III, Ed.; Plenum: New York, **1976**; p.1.
(e) Hay, P. J.; Wadt, W. R. *J. Chem. Phys.* **1985**, *82*, 270.
(f) Wadt, W.R.; Hay, P.J. *J. Chem. Phys.* **1985**, *82*, 284.
(g) Hay, P.J.; Wadt. W. R. *J. Chem. Phys.* **1985**, *82*, 299.
35. Cui, Q.; Musaev, D. G.; Svensson, M.; Morokuma, K. *J. Phys. Chem.*, **1996**, *100*, 10936.
36. Humbel, S.; Sieber, S.; Morokuma, K. *J. Chem. Phys.* **1996**, *105*, 1959.
37. Svensson, M.; Humbel,S.; Morokuma, K. *J. Chem. Phys.* **1996**, *105*, 3654.
38. Coitiño, E.L.; Truhlar, D. G.; Morokuma, K. *Chem. Phys. Lett.* **1996**, *259*, 159.
39. Noland, M.; Coitiño, E.L.; Truhlar, D.G. *J. Phys. Chem. A* **1997**, *101*, 1193.
40. Matsabura, T.; Maseras, F.; Koga, N.; Morokuma, K. *J. Phys. Chem.* **1996**, *100*, 2573.
41. Maseras, F.; Morokuma, K. *J. Comput. Chem.* **1995**, *16*, 1170.
42. Frisch, M. J.; Trucks, G. W.; Schlegel, H. B.; Gill, P. M. W.; Johnson, B. G.; Robb, M. A.; Cheeseman, J. R.; Keith, T.; Petersson, G. A.; Montgomery, J. A.; Raghavachari, K.; Al-Laham, M. A.; Zakrzewski, V. G.; Ortiz, J. V.; Foresman, J. B.; Cioslowski, J.; Stefanov, B. B.; Nanayakkara, A.; Challacombe, M.; Peng, C. Y.; Ayala, P. Y.; Chen, W.; Wong, M. W.; Andres, J. L.; Replogle, E. S.; Gomperts, R.; Martin, R. L.; Fox, D. J.; Binkley, J. S.; Defrees, D. J.; Baker, J.; Stewart, J. P.; Head-Gordon, M.; Gonzalez, C.; Pople, J. A. *Gaussian 94, Revision C.3*, Gaussian, Inc., Pittsburgh PA, 1995.
43. Froese, R. J. D.; Morokuma, K. *Chem. Phys. Lett*, **1996**, *263*, 393; Dapprich, S.; Komaromi, I.; Byun, K. S.; Holthausen, M. C.; Morokuma, K.; Frisch, M. J. *J. Mol. Struct.* (*THEOCHEM*), to be submitted.
44. Hawkins, G. D.; Liotard, D. A.; Cramer, C. J.; Truhlar, D. G. *AMPAC version 5.4ml*, University of Minnesota, Minneapolis, **1997**. This package is a set of modifications to *AMPAC version 5.4*, Semichem, Inc., Shawnee, Kansas to incorporate the SM5.2R solvation model for MNDO/d and other semiempirical methods.
45. Zhu, T.; Giesen, D. J.; Liotard, D. A.; Stahlberg, E. A.; Hawkins, G. D.; Chambers, C. C.; Cramer, C. J.; Truhlar, D. G. *DGSOL version 4.0ml*, University of Minnasota, Minneapolis, 1997. This package is a set of revisions to *DGAUSS version 4.0*, Oxford Molecular Group, UK to incorporate the SM5.42R solvation model for DFT. For a more complete description of *DGAUSS* see Andzelm, J.; Wimmer, E. J. Chem. Phys. **1992**, *96*, 1280.
46. Chambers, C. C.; Hawkins, D. G.; Cramer, C. J.; Truhlar, D. G. *J. Phys. Chem.* **1996**, *100*, 16385.
47. Giesen, D. J.; Cramer, C. J.; Truhlar, D. G. *J. Org. Chem.* **1996**, *61*, 8720.
48. Hawkins, G. D.; Cramer, C. J.; Truhlar, D. G. *J. Phys. Chem B.* **1997** *101*, 7147.
49. Zhu, T.; Li, J.; Hawkins, G. D.; Cramer, C. J.; Truhlar, D. G., to be published.
50. Cramer, C. J.; Truhlar, D. G. *J. Am. Chem. Soc.* **1991**, *113*, 8305.
51. Cramer, C. J.; Truhlar, D. G. *J. Comput.-Aided Molec. Des.* **1992**, *6*, 629.
52. Giesen, D. J.; Cramer, C. J.; Truhlar, D. G. *J. Phys. Chem.* **1995**, *99*, 7137.
53. Giesen, D. J.; Hawkins, G. D.; Chambers, C. C.; Lynch, G. C.; Rossi, I.; Storer, J. W.; Liotard, D. A.; Cramer, C. J.; Truhlar, D. G. *AMSOL version 6.1.1*, University of Minnesota, Minneapolis, **1997**.
54. Cramer, C. J.; Truhlar, D. G. in *Solvent Effects and Chemical Reactivity*; Tapia, O., Bertrán, J., Eds.; Kluwer: Dordrecht, **1996**; p. 1.
55. Thiel, W.; Voityuk, A. A. *Int. J. Quantum Chem.* **1992**, *44*, 807.
56. Thiel, W.; Voityuk, A. A. *Theor. Chim. Acta* **1996**, *93*, 315.
57. Thiel, W.; Voityuk, A. A. *J. Phys. Chem.* **1996**, *100*, 616.

58. Thiel, W., private communication of Zr parameters.
59. Becke, A. D. *Phys. Rev. A.* **1988**, *38,* 3088. Perdew, J. P.; Burke, K.; Wang, Y. *Phys. Rev. B* **1996**, *54*, 16533.
60. Easton, R. E.; Giesen, D. J.; Welch, A.; Cramer, C. J.; Truhlar, D. G. *Theor. Chim. Acta* **1996**, *93*, 281.
61. Li, J.; Zhu, T.; Cramer, C. J.; Truhlar, D. G. *J. Phys. Chem.* A, **1998**, *102*, 1820.
62. Chuang, Y.-Y.; Cramer, C. J.; Truhlar, D. G. *Int. J. Quantum Chem.*, to be published.